Correlation between band structure and magneto-transport properties in far-infrared detector modulated nanostructures superlattice

R. Morghi[a], A. Nafidi[a*], M. Braigue[a], H. Chaib[a], J. Hemine[a], A. Tirbiyine[a], B. Er-Raha[a], M. Garcia Enrique[b] and M. d'Astuto[c]

[a]*Group of Condensed Matter Physics, Department of Physics, Faculty of Sciences, P.O. Box 8106 Dakhla, University Ibn Zohr, 80000 Agadir, Morocco*

[b]*Dto. de Física de la Materia Condensada, Universidad Autónoma de Madrid, 28049 Madrid, Spain*

[c]*IMPMC, CNRS UMR7590 UPMC, 140 rue de Lourmel, 75015 Paris, France*

Abstract: We report here carrier's magneto-transport properties and the band structure results for II-IV semiconductors. HgTe is a zero gap semiconductor when it is sandwiched between CdTe layers to yield to a small gap HgTe/CdTe superlattice which is the key of an infrared detector. Our sample, grown by MBE, had a period d (100 layers) of 18 nm (HgTe) / 4.4 nm (CdTe). Calculations of the spectra of energy $E(k_z)$ and $E(k_p)$, respectively, in the direction of growth and in the plane of the superlattice were performed in the envelope function formalism. The angular dependence of the transverse magnetoresistance follows the two-dimensional (2D) behavior with Shubnikov-de Haas oscillations. At low temperature, the sample exhibits p type conductivity with a hole mobility of 900 cm²/V.s. A reversal the sign of the weak-field Hall coefficient occurs at 25 K with an electron mobility of 3 10^4 cm^2/Vs. In intrinsic regime, the measured $E_g \approx 38$ meV agrees with calculated $E_g(\Gamma,300\ K) = 34$ meV which coincide with the Fermi level energy. The formalism used here predicts that this narrow gap sample is semi metallic, quasi-two-dimensional and far-infrared detector.

Keywords: Band structure, Envelope function formalism, Magnetoresistance, Hall effect, HgTe/CdTe superlattice, Infrared detector, Narrow gap, quasi-two-dimensional system.

Corresponding author: E-mail: nafidi21@yahoo.fr, Phone: +212 664 168 519, Fax: +212 528 220 100

I. Introduction

The work of Essaki and Tsu in 1970 [1] caused a big interest in the study of superlattices made from alternating layers of two semiconductors. The development of molecular beam epitaxy (MBE) was successfully applied to fabricate different quantum wells and superlattices. Among them, III-V superlattices ($Ga_{1-x}Al_xAs$-GaAs [1-2] - type I), IV-IV (InAs/GaSb [3] - type II) and later II-VI superlattice (HgTe/CdTe [4] - type III). HgTe and CdTe crystallize in zinc–blend lattice respectively. The lattice-matching within 0.3% results in a small interdiffusion between HgTe and CdTe layers at low temperature near 200°C by MBE. HgTe is a zero gap semiconductor (due to the inversion of relative positions of Γ_6 and Γ_8 edges [5]) when it is sandwiched between the wide gap semiconductor CdTe (1.6 eV at 4.2 K) layers yield to a small gap HgTe/CdTe superlattice which is the key of an infrared detector.

A number of papers have been published devoted to the band structure of this system [4] as well as its magnetooptical and transport properties [6]. In this paper we report the band structure and magneto-transport results in semi metallic HgTe/CdTe superlattice grown by molecular beam epitaxy.

II. Experimental Techniques

The HgTe/CdTe superlattice was grown by MBE on a [111] CdTe substrate at 180 °C. The sample (100 layers) had a period $d = d_1+d_2$ where d_1(HgTe)=18 nm and d_2(CdTe) = 4.4 nm. It was cut from the epitaxial wafer, had typical sizes of 5×1×1 mm^3. The ohmic contacts were obtained by chemical deposition of gold from a solution of tetrachloroauric acid in methanol after a proper masking to form the Hall crossbar. Carrier transport properties were studied in the temperature range 1.5-300 K in magnetic field up to 8 Tesla. Conductivity, Hall effect [7], angular dependence of the transverse magnetoresistance and the Hall voltage with respect to the magnetic field were measured. The measurements at weak magnetic fields (up to 1.2 T) were performed in standard cryostat equipment. The measurements of the magnetoresistance were done under a higher magnetic field (up to 8 Tesla). The sample was immersed in a liquid helium bath, in the center of a superconducting coil. Rotating samples with respect to the magnetic field direction allowed us to study the angular dependence of the magnetoresistance and Hall voltage.

III. Theory of electronic bands

Calculations of the spectra of energy $E(k_z)$ and $E(k_p)$, respectively, in the direction of growth and in plane of the superlattice; were performed in the envelope function formalism [4,6] with a valence band offset Λ between heavy holes bands edges of HgTe and CdTe of 40 meV determined by the magneto-optical absorption experiments [8].

The general dispersion relation of the light particle (electron and light hole) subbands of the superlattice is given by the expression [4]:

(1)

$$\cos k_z(d_1+d_2) = \cos(k_1 d_1)\cos(k_2 d_2) - \frac{1}{2}\left(\xi - \frac{1}{\xi}\right)\sin(k_1 d_1)\sin(k_2 d_2)$$

Where the subscripts 1 and 2 refer, respectively, to HgTe and CdTe. k_z is the superlattice wave vector in the direction parallel to the growth axis. The two-dimensional wave vector $k_p(k_x,k_y)$ describes the motion of particles perpendicular to k_z. Here:

$$\xi = \frac{k_1}{k_2}\, r \qquad r = \frac{E-\varepsilon_2}{E+|\varepsilon_1| - \Lambda} \tag{2}$$

E is the energy of the light particle in the superlattice measured from the top of the Γ_8 valence band of bulk CdTe, while ε_i (i =1 or 2) is the interaction band gaps $E(\Gamma_6) - E(\Gamma_8)$ in the bulk HgTe and CdTe respectively. At given energy, the two–band Kane model [9] gives the wave vector $(k_i^2+k_p^2)$ in each host material:

$$\left.\begin{aligned} \frac{2}{3}P^2\hbar^2(k_1^2+k_p^2) &= (E-\Lambda)(E-\Lambda+|\varepsilon_1|) && \text{for HgTe,}\\ \frac{2}{3}P^2\hbar^2(k_2^2+k_p^2) &= E(E-\varepsilon_2) && \text{for CdTe} \end{aligned}\right\} \tag{3}$$

P is the Kane matrix element given by the relation:

$$\frac{2P^2}{3|\varepsilon_1|} = \frac{1}{2m^*} \tag{4}$$

Where $m^* = 0.03\ m_0$ is the electron cyclotron mass in HgTe [5]. For a given energy E, a superlattice state exists if the right-hand side of Eq. (1) lies in the range [-1,1] that implies $-\pi/d \le k_z \le \pi/d$ in the first Brillion zone.

The heavy hole subbands of the superlattice are given by the same Eq. (1) with:

$$\xi = \frac{k_1}{k_2}\, r \qquad and \qquad r = 1$$

$$-\frac{\hbar^2(k_1^2+k_p^2)}{2\,m^*_{HH}} = E - \Lambda \qquad \text{for HgTe} \tag{5}$$

$$-\frac{\hbar^2(k_1^2+k_p^2)}{2\,m^*_{HH}} = E \qquad \text{for CdTe}$$

$m^*_{HH} = 0.3\ m_0$ [5] is the effective heavy hole mass in the host materials.

The energy E as a function of d_2, at 4.2 K, in the center Γ of the first Brillouin zone and for $d_1 = 4.1\ d_2$, is shown in Fig. 1.

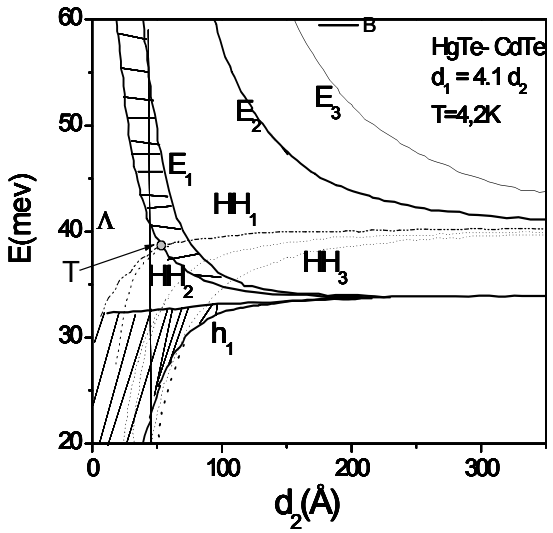

Figure 1: Energy position and width of the conduction (E_n), heavy-hole (HH_n), and the first light-hole (h_1) subbands calculated at 4.2 K in the center Γ of the first Brillouin zone as a function of layer thickness d_2 for HgTe/CdTe superlattice with $d_1 = 4.1\ d_2$, where d_1 and d_2 are the thicknesses of the HgTe and CdTe layers, respectively. T is the point of the transition semiconductor-semimetal.

The case of our sample (d_2 = 44Å) is indicated by the vertical solid line. Here the cross-over of E_1 and HH_1 subbands occurs. d_2 controls the superlattice band gap $Eg = E_1\text{-}HH_1$. For weak d_2 the sample is semiconductor with a strong coupling between the HgTe wells. At the point T(d_2 = 53.7 Å, E= 38.7 meV) the gap goes to zero with the transition semiconductor- semimetal. When d_2 increases, E_1 and h_1 states drops in the energy gap [0, Λ] and become interface state with energy

$$E_1 = \Lambda\varepsilon_2/(|\varepsilon_1|+\varepsilon_2) = 34 \text{ meV}$$

for infinite d_2. Then the superlattice has the tendency to become a layer group of isolated HgTe wells and thus assumes a semimetallic character. The ratio d_1/d_2 governs the width of superlattice subbands (i.e. the electron effective mass). A big d_1/d_2, as in our case,

moves away the material from the two-dimensional behavior.

In Fig. 2 we can see that the band gap $E_g(\Gamma)$ increases, presents a maximum at 0 meV and decreases when the valence band offset Λ between heavy hole band edges of HgTe and CdTe increase. For each Λ, $E_g(\Gamma)$ increases with T. Our chosen value of 40 meV is indicated by a vertical dashed line. This offset agrees well with our experimental results contrary to 0 meV used by Bastard [4] and 360 meV given by Johnson [8]. The later offset give a zero gap whereas, in intrinsic regime, our measured Eg ≈ 38 meV agree with calculated $E_g(\Gamma,300\ K) = 34$ meV.

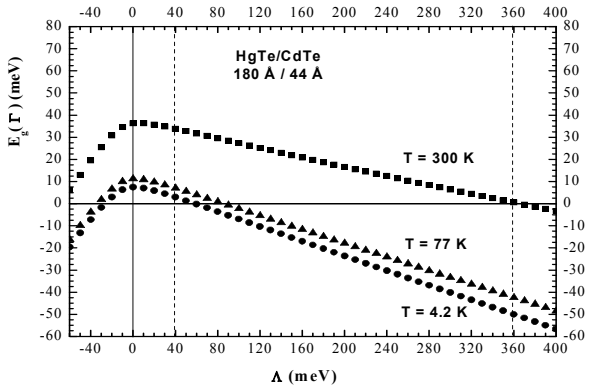

Figure 2: The band gap E_g (Γ), in the center Γ of the first Brillouin zone, as function of temperature and valence band offset Λ between heavy holes bands edges of HgTe and CdTe for the investigated HgTe/CdTe superlattice.

Fig. 3 shows the spectra of energy $E(k_z)$ and $E(k_p)$, respectively, in the direction of growth and in plane of the superlattice at 4.2 K. Along $E(k_p)$, E_1 and h_1 increase with k_p whereas HH_n decreases. This yields to an anti-crossing of HH_1 and h_1 at k_p=0.0168 Å^{-1}. The gap is $E_g(\Gamma,4.2\ K) = 3$ meV.

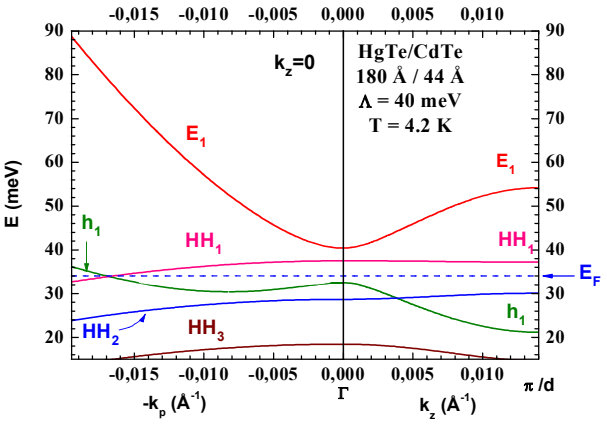

Figure 3: Calculated bands along the wave vector k_z (a) and in plane $k_p(k_x,k_y)$(b), of the HgTe/CdTe superlattice at 4.2 K. E_F is the energy of Fermi level.

Please note that E_F(4.2 K) =34 meV= E_I and then the conduction is assumed by heavy and light holes. As seen in Fig. 4, along k_z and k_p the light particles (electrons and light holes) subbands are not parabolic whereas the heavy hole subbands are parabolic.

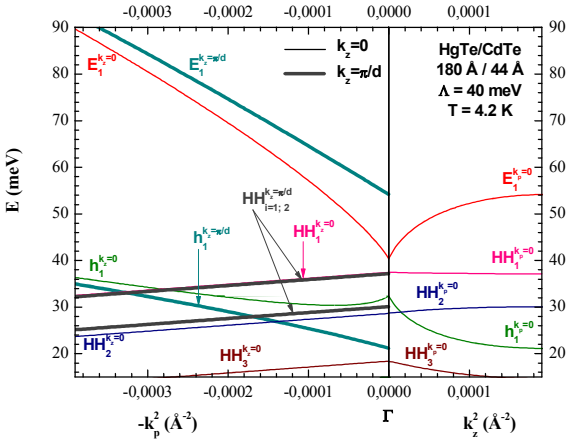

Figure 4: Calculated bands as a function of k_z^2 and k_p^2 of the HgTe/CdTe superlattice at 4.2 K.

For an anisotropic medium, such as the HgTe/CdTe superlattices, the effective mass is a tensor and its elements along μ and ν directions are given by the following expression [10]:

$$\left(\frac{1}{m^*}\right)_{\mu\nu} = \frac{1}{\hbar^2}\frac{\partial^2 E_{k_{\mu\nu}}}{\partial k_\mu \partial k_\nu} \qquad (6)$$

By carrying out second derivative of the energy E_1, h_1 and HH_1 along k_z and k_p in Fig. 3 we calculated the effective mass bands in Fig. 5. Along kp, the effective mass of heavy holes m^*_{HH1}= -0.300 m_0 and the effective mass of electrons m^*_{E1} increases from 0.011 m_0 to 0.080 m_0 whereas the effective mass of the light holes h_1 deceases from 0.140 m_0 by half to a minimum of 0.074 m_0. After it increases and diverges at k_p = 0.003 Å^{-1} assuming an electronic conduction. After it increases to -0.034 m_0 at the center Γ of the first Brillouin zone assuming a light hole conduction.

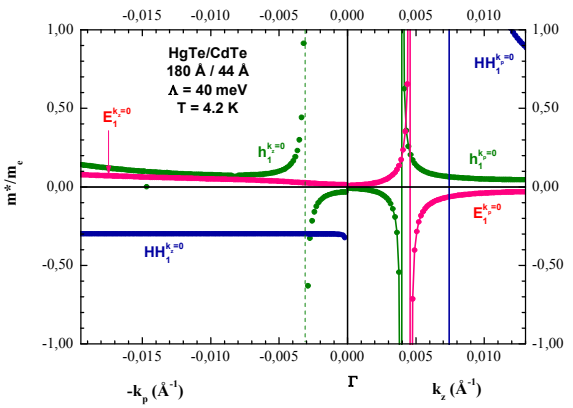

Figure 5: Calculated relative effective mass bands along the wave vector k_z and in plane k_p of the HgTe/CdTe superlattice at 4.2 K.

Using the value of ε_1 and ε_2 at 4.2 K, 77 K and 300 K [11] and taking P temperature independent, this is

supported by the fact that from eq.(4) $P \approx \varepsilon_G(T)/m^*(T) \approx$ cte, we get the temperature dependence of the band gap E_g, in the center Γ of the first Brillouin zone in Fig. 6.

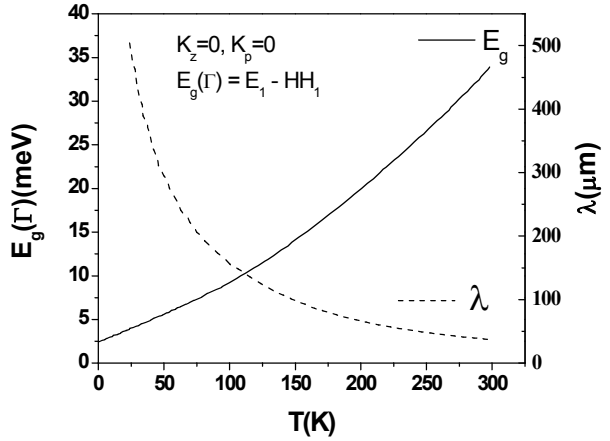

Figure 6: Temperature dependence of the band gap E_g and cut-off wavelength, at the center Γ of the first Brillouin zone, in the investigated HgTe/CdTe superlattice.

Note that E_g increases from 3.6 meV at 4.2 K to 34 meV at 300K. We calculated the detection cut-off wave length by the relation:

$$\lambda(\mu m) = \frac{1240}{E_g(meV)} \qquad (7)$$

In the investigated temperature range $40\,\mu m \le \lambda \le 500\,\mu m$ situates our sample as a far infrared detector.

IV. Experimental Results and discussion

The transverse magnetoresistance ρ/ρ_0, in Fig. 7, follows the two-dimensional (2D) dependence with manifestation of the beginning of the Shubnikov-de Haas oscillations (with a weak $[(\Delta\ \rho/\rho_0)_{max} = 0.2]$). However, over the entire investigated magnetic field range, a non-vanishing magnetoresistance is observed when the field is parallel to the plane. This can be due to the inter-diffusion between HgTe well (great d_1/d_2 and small d_2) and/or to the widening of carriers subbands under the influence of the magnetic field along $E(k_p)$ while the Hall voltage V_H goes to zero at this configuration in Fig. 8. This suggests quasi two-dimensional conductivity behavior (between three-dimensional (3D) and two-dimensional (2D).

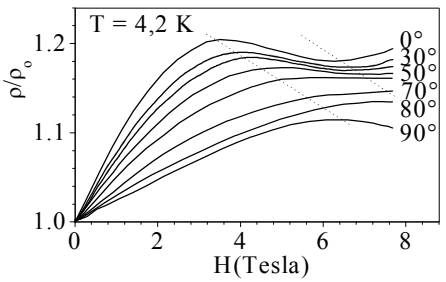

Figure 7: Transverse magnetoresistance of the sample, at various angles between the magnetic field and the normal to the HgTe/CdTe superlattice surface, at 4.2 K.

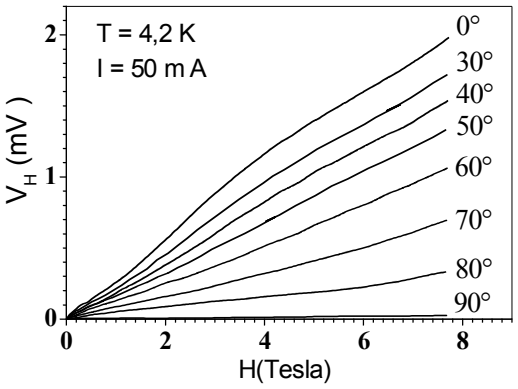

Figure 8: Field dependence of Hall voltage, at various angles between the magnetic field and the normal to the HgTe/CdTe superlattice surface, at 4.2 K.

At low temperature, the sample exhibits p type conductivity with a hole mobility $\mu_p \approx 900$ cm²/V.s. As seen in Fig. 9, a reversal of the sign of the weak-field Hall coefficient R_H occurs at 25 K. It may be attributed to trapping of carrier charges in intrinsic state E_I. Such a reversal of the sign of the Hall voltage may be inferred by the existence of at least two types of carriers, which suggests a semimetallic character of the conduction mechanism.

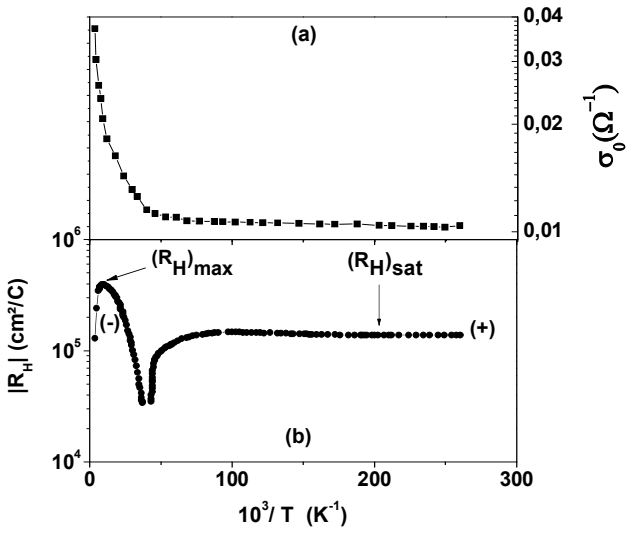

Figure 9: Temperature dependence of the conductivity (a) and weak-field Hall coefficient (b), in the investigated HgTe/CdTe superlattice.

The Hall constant at weak field in Fig. 9 is described by the formula:

$$(R_H)_w = \frac{1}{|e|}\frac{p\text{-}nb^2}{(p+nb)^2} \quad \text{where} \quad b = \frac{\mu_n}{\mu_p} \tag{8}$$

At low temperature in the saturation regime:

$$(R_H)_{sat} = \frac{1}{|e|\,p} \tag{9}$$

Near the intrinsic regime, the Hall constant is given by:

$$(R_H)_{\max} = \frac{(b-1)^2}{|e|\,4bp} \tag{10}$$

This results in the ratio:

$$\frac{4(R_H)_{\max}}{(R_H)_{sat}} = \frac{(b-1)^2}{b} \approx b = 32 \tag{11}$$

Eq. (8) implies for RH = 0:

$$b^2 = 1024 = \frac{p}{n} \tag{12}$$

This implies an electron mobility of $\mu n = 3\times10^4$ cm²/V.s. Such a low value of the electron mobility can be connected, from the one side, with the superlattice electron effective mass which is much higher than that of the bulk material [12] and, from the other side, with different types of imperfections of the investigated structures, including strong compensation.

From Eq. (3) we have:

$$\frac{2}{3}P^2\hbar^2k_F^2 = E_F(E_F - E_g) \tag{13}$$

We extract the Fermi level energy:

$$E_F = \frac{E_g}{2} \pm \sqrt{\left(\frac{E_g}{2}\right)^2 + \frac{2}{3}P^2\hbar^2k_F^2} \tag{14}$$

Where the Fermi wave vector is $k_F(3D) = (3\pi^2 p)^{1/3}$ and $k_F(2D) = (2\pi p)^{1/2}$, respectively for three-dimensional and two-dimensional motion of carriers charges. Here we have chosen the minus sign because the sample is p-type at low temperature. Fig. 10 shows that the band gap and the 3D Fermi level energy increase with temperature whereas 2D Fermi level energy and HH_i band energy remain constant. In all cases the conductivity is assumed by light and heavy holes. So we have quasi-two-dimensional and semimetallic conductivity.

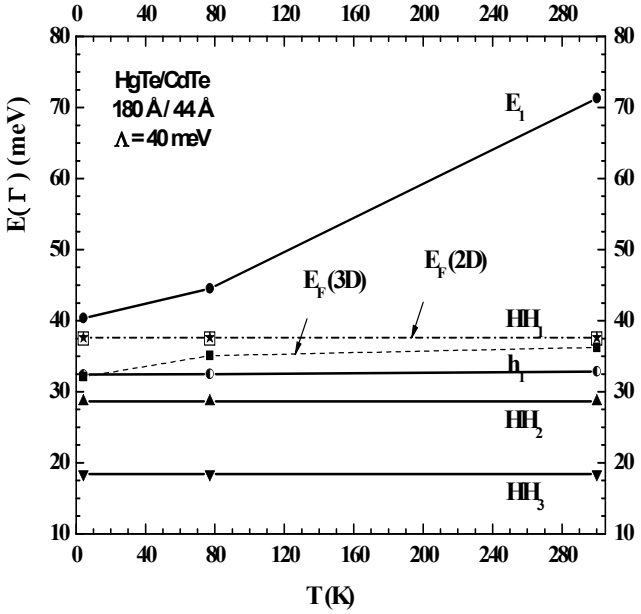

Figure 10: Temperature dependence of the energy for the three-dimensional (3D) and two-dimensional (2D) Fermi levels in the investigated HgTe/CdTe superlattice.

V. Conclusions

The formalism used here predicts that the system is semimetallic when the HgTe to CdTe thickness ratio d_1/d_2 is greater than 4. In our case, d_1/d_2 = 4.1 and $E_g(\Gamma,4.2\text{ K})$ = 3 meV corresponding to thermal energy necessary to change the sign of $R_H(1/T)$. In intrinsic regime, the measurements indicates $E_g \approx 38$ meV in good agreement with calculated E_g (Γ,300 K) =34meV and E_F (4.2K)=E_1. In spite of it, the sample exhibits the features typical for the semimetallic conduction mechanism, which agree well with the overlap between carrier subbands in $E(k_p)$ with a quasi-two-dimensional behavior and is a far-infrared detector. The theoretical and magnetotransport parameters are in good agreement for our sample with narrow gap near the point T. Note that we had observed a p-type conduction mechanism in the medium-infrared detector, narrow gap and two-dimensional HgTe/CdTe (5.6 nm / 3 nm) superlattice [13-14]. Measurements performed by us on others' samples indicate an improvement of quality of the material, manifested by higher mobility.

VI. References

[1] L. Esaki and R. Tsu, "Superlattice and negative differential conductivity in Semiconductors", IBM J. Res. Development, 61-65 (1970).

[2] R. Dingle, A. C. Gossard, and W. Wiegmann, "Direct Observation of Superlattice Formation in a Semiconductor Heterostructure", Phys. Rev. Lett. **34**, 1327-1330 (1975).

[3] H. Sakaki, L. L. Chang, G. A. Sai-Halasz, C. A. Chang, and L. Esaki, "Two-dimensional electronic structure in InAs-GaSb superlattices", Solid State Communications **26**, 589-592 (1978).

[4] G. Bastard, "Theoretical investigations of superlattice band structure in the envelope-function approximation", Phys. Rev. B **25**, 7584-7597 (1982).

[5] J. Tuchendler, M. Grynberg, Y. Couder, H. Thomé, and R. Le Toullec, "Submillimeter Cyclotron Resonance and Related Phenomena in HgTe", Phys. Rev. B **8**, 3884-3894 (1973).

[6] Ab. Nafidi, A. El Kaaouachi, H. Sahsah, and Ah. Nafidi, "Band structure and magneto-transport in HgTe/CdTe superlattice", International Conference on Theoretical Physics (HT 2002), Paris, France 22-27 July, 274-275 (2002).

[7] Ab. Nafidi, A. El Kaaouachi, Ah. Nafidi, J.P. Faurie, A. Million, and J. Piaguet, **"**Some Transport Properties of HgTe/CdTe Superlattices", Physica Status Solidi (b) **229**, 573-576 (2002).

[8] N. F. Johnson, P. M. Hui, and H. Ehrenreich, "Valence-Band-Offset Controversy in HgTe/CdTe Superlattices. A Possible Resolution", Phys. Rev. Lett. **61**, 1993-1995 (1988).

[9] Evan O. Kane, "Band structure of indium antimonide", Journal of Physics and Chemistry of Solids **1**, 249-261 (1957).

[10] C. Kittel, "Introduction to solid state physics", 3rd edition, John Wiley and Sons, Inc, New York, 333 (1971).

[11] M. H. Weiler, "Semiconductors and Semimetals", edited by R. K. Willardson and A. C. Beer (Academic, New York), vol. 16, 119 (1981).

[12] D. L. Smith, T. C. McGill, and J. N. Schulman, "Advantages of the HgTe-CdTe superlattice as an infrared detector material", Appl. Phys. Lett. **43**, 180 (1983).

[13] Ab. Nafidi, A. EL Abidi, A. El Kaaouachi, and Ah. Nafidi, "Electronic Band Structure and New Magneto-transport Properties in p-type Semiconductor Medium-infrared HgTe / CdTe Superlattice**",** AIP Conference Proceedings, Volume 772, 1001-1002 (2004).

[14] A. Nafidi, A. El Abidi, and A. El Kaaouachi, "Seebeck and Shubnikov-de Haas Effects in a Two-Dimensional p-type HgTe/CdTe Superlattice"**,** AIP Conference Proceedings, Volume 850, 1359-1360 (2006).